

This is the accepted version of the article:

Guardingo, M.; Esplandiu, M.J.; Ruiz-Molina, D.. Synthesis of polydopamine at the femtoliter scale and confined fabrication of Ag nanoparticles on surfaces. *Chemical Communications*, (2014). 50. 83: 12548 - . 10.1039/c4cc02500h.

Available at: <https://dx.doi.org/10.1039/c4cc02500h>

Synthesis of polydopamine at the femtoliter scale and confined fabrication of Ag nanoparticles on surfaces

Cite this: DOI: 10.1039/x0xx00000x

M. Guardingo,^a M. J. Esplandiu^a and D. Ruiz-Molina^{a,*}

Received 00th January 2012,

Accepted 00th January 2012

DOI: 10.1039/x0xx00000x

Nanoscale polydopamine motives are fabricated on surfaces by deposition of precursor femtolitre droplets with an AFM tip and used as confined reactors to fabricate Ag nanoparticles patterns by in-situ reduction of an Ag⁺ salt.

The controlled engineering of functional nanoarchitectures on surfaces is a challenging area of growing interest and technological relevance in chemistry and materials science.^{1,2} However, its full expansion is limited by the substrate specificity of most known methods.^{3,4} In this context, polydopamine (PDA) emerges as a virtually universal and multifunctional coating inspired by the adhesive proteins found in mussels. Since first reported by Messersmith and co-workers in 2007,⁵ the number of publications exploiting the versatility of polydopamine and other structurally related materials has been growing steadily.^{6,7} So far, PDA has been micro/nano-structured by photolithography,⁸ microfluidics⁹ colloidal lithography¹⁰ and microcontact printing¹¹ in a variety of substrates and further proved to retain its properties by creating cell, protein or metallic nanoparticle patterns. However, the use of direct-writing nanolithographies that avoid the use of stamps and masks and do not require any modification of the substrates¹² has not been reported to date. Herein we describe the use of AFM tip to directly deliver femtolitre droplets of a mildly basic dopamine hydrochloride solution onto specific regions of a surface. Each droplet acts as a reactor vessel confined at the nanoscale, where the polymerization takes place.¹³ Following this approach we have successfully fabricated PDA nanoarrays on Si/SiO₂ substrates and tested the interfacial properties of the deposited material by means of force/distance curves. The results show that the nanostructures retain the chemical properties of PDA with improved adhesive character. Moreover, the same arrays were successfully used for the fabrication of Ag nanoparticles by in-situ reduction of a silver salt and their conductive properties studied upon insertion of gold electrodes by conventional electron beam lithography. The whole process is schematically depicted in Figure 1.

Our first efforts were directed to fabricate bulk PDA coatings on Si wafers following a methodology previously described.⁵ In a typical experiment, clean Si (bearing a native layer of SiO₂, from here on Si/SiO₂) substrates were immersed in a solution of dopamine hydrochloride in 10 mM Tris-HCl buffer (2mg/mL, pH 8.59) and kept in vertical orientation while stirring for a given time (1h or overnight). The substrates were then rinsed with copious amounts of

Milli-Q water and dried under a N₂ stream. Examination of the as-prepared coatings by tapping mode AFM revealed a rough topography and coating thickness of around 10 nm for the sample functionalised for 1h and 35 nm when it was kept in the PDA solution overnight (see Figure 2). Concurrently, the structuration of PDA on surface was achieved by direct-write AFM lithography. In a typical experiment, a basic solution of dopamine hydrochloride in Tris-HCl buffer was obtained and immediately used to coat an AFM tip.

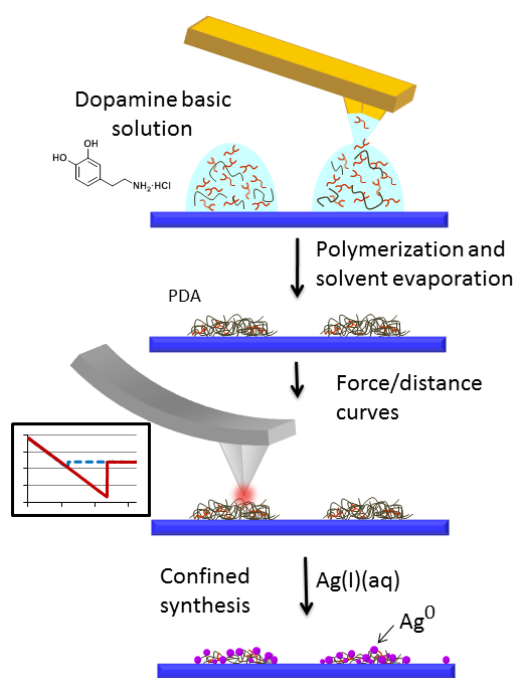


Fig. 1 Schematic representation of the fabrication of polydopamine at the femtolitre scale. A basic solution of dopamine is deposited on a surface through an AFM tip while polymerizing. Afterwards, the interfacial properties (adhesion and redox activity) of the deposited material are tested.

The coated tip was then brought into contact with the surface and drops of controlled size were deposited to create PDA dot-like

feature arrays. To avoid fast evaporation of the dopamine solution, the ambient humidity during the lithographic process was maintained at $\sim 70\%$ and the substrates were kept under these conditions for approximately 2h (for more experimental details see Supporting Information, S1). The obtained structures were characterized by optical microscopy and tapping mode AFM, revealing structures that were reproducible and uniform in size (Figure 2 and Supporting Information, S2-S4). The height profile analysis of the dot-like features reveals that the structures had an average diameter around $1\ \mu\text{m}$ and a typical height of 20 nm. Further control over parameters such as the ink loading of the tip or tip-substrate contact time allowed us to adjust the dimensions of the motifs and obtain dot-like features with diameters as small as 500 nm (See Supporting Information, S3). The deposition process could also be repeated several times to create patterns over extended areas. Switching the writing mode from static to dynamic also allowed us to obtain, not only dot arrays, but also lines and more complex shapes with reduced heights (See Supporting Information, S4).

Once the arrays were fabricated, an AFM tip was used to study the adhesive properties of the motifs by means of Force-distance (F-d) curves. This technique has already been successfully used to give new insights on the adhesive properties of catechols by means of single-molecule mechanics¹⁴ and more recently by ourselves on a self-assembled monolayer of outward-facing catechol moieties.¹⁵ The jump-out of the tip that occurs when it is retracted from the surface is directly related to the adhesion or, more precisely, the interaction of the tip with the substrate. For this, force-distance curves were recorded both inside and outside of the dots. The exact location of the dot-like features was determined by previously

scanning the surface. To avoid tip contamination during this process the cantilever deflection was kept as low as possible and the contact time of the tip with the surface was minimized. F-d curves on the PDA dot-like features performed on a variety of lithographies exhibit a low dispersion of values with an average force of 16 nN (see Figure 2), independently of the feature dimensions. This average value is slightly higher than that obtained for the thin PDA coating (10 nm) with an adhesion force clearly centred at 11 nN. The results obtained for the thicker coating (35 nm) presented a high statistical dispersion whereupon a clear adhesion force value could not be extracted (see Figure 2). This fact can be tentatively attributed to the diminished homogeneity of the thicker coating, which becomes then more deformable and softer with a larger tendency to retain water.^{16,17}

The ability of PDA nanoarrays to in-situ reduce Ag^+ ions to metallic Ag was also checked. Before that, and following previous approaches, model bulk Si/SiO₂ substrates were coated with PDA overnight and then rinsed with water and dried in a N₂ stream.^{18,19} Afterwards they were immersed in a AgNO₃ solution (50 mM in Milli-Q water) without stirring for 24h and rinsed with copious amounts of water. Examination of the samples by FE-SEM showed the formation of a considerable amount of Ag particles on the polymeric coating (See Supporting Information, S5). According to Ball et al. reduction of Ag^+ is not due to 5,6-dihydroxyindole, one of the main component of PDA,²⁰ but rather to the presence of free dopamine in the polymer, as recently confirmed by Lee et al.²¹ However, reproduction of the same experimental conditions on the PDA nanoarrays resulted in the loss of the motifs (See Supporting Information, S6).

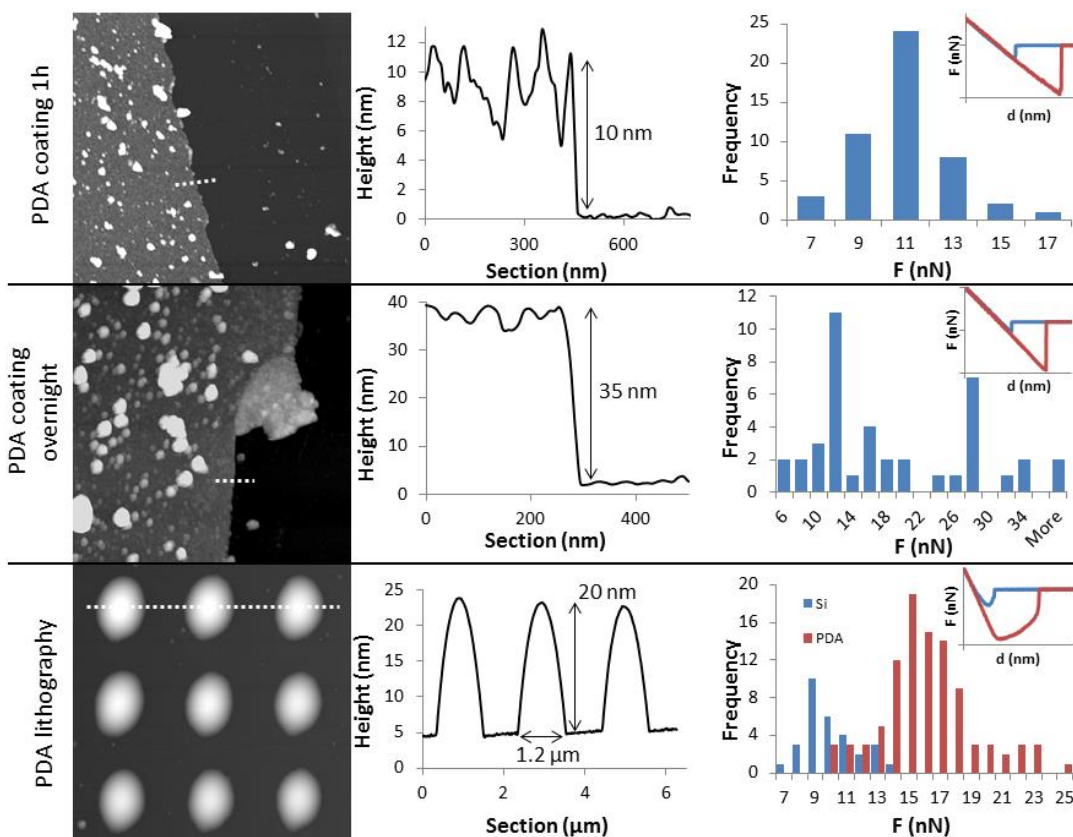


Fig. 2 AFM tapping mode images (left), profiles corresponding to dashed lines in images (centre) and histograms generated from F-d curves (right). For the PDA coatings, a scratch was intentionally made on the polymer in order to measure their thickness. A representative F-d curve of each system is presented as an inset in the histograms.

This limitation was finally overcome by decreasing the incubation time. Therefore, successful reduction of Ag^+ on specific locations was achieved by immersing a PDA-patterned substrate in a 10 mM solution of AgNO_3 and heating it in an oven at 60°C for 1h.²² Figure 3C shows HR-SEM images of a dot array in which each one of the features contains a number of silver particles while maintaining the order and lateral resolution of the dot-like structures generated by AFM lithography. The silver particles are clearly observed in Figure 3D. Formation of Ag on the deposited material was confirmed by EDX analysis (See Supporting Information, S7).

The rather continuous and highly homogeneous metallic layer obtained in the larger dots allowed us to measure the electrical resistivity of the islands by a 2-point conductivity method. For this, conventional electron beam lithography and lift-off methods were used to deposit two small titanium/gold electrodes on top of the silver/PDA structures. The gap between these two small electrodes was about $10\ \mu\text{m}$. These small electrodes were connected to big gold pads on which the two point contact methodology was performed. Experimental results showed conductivity as low as $2.2 \times 10^{-3}\ \text{ohm.m}$ at room temperature (See Supporting Information, S8).

In summary, AFM-assisted lithography is a suitable technique to accurately deposit the archetypal PDA on surfaces in the shape of femtolitre sized droplets without any previous functionalization, while controlling the deposited volume and the exact location. Interestingly the PDA motives proved to retain the chemical reactivity and adhesive behaviour, opening new venues to the manufacture of nanoscale devices by green synthesis approaches based on PDA. As a proof-of-concept, the fabrication of Ag nanoparticles by in-situ reduction of a silver salt is reported.

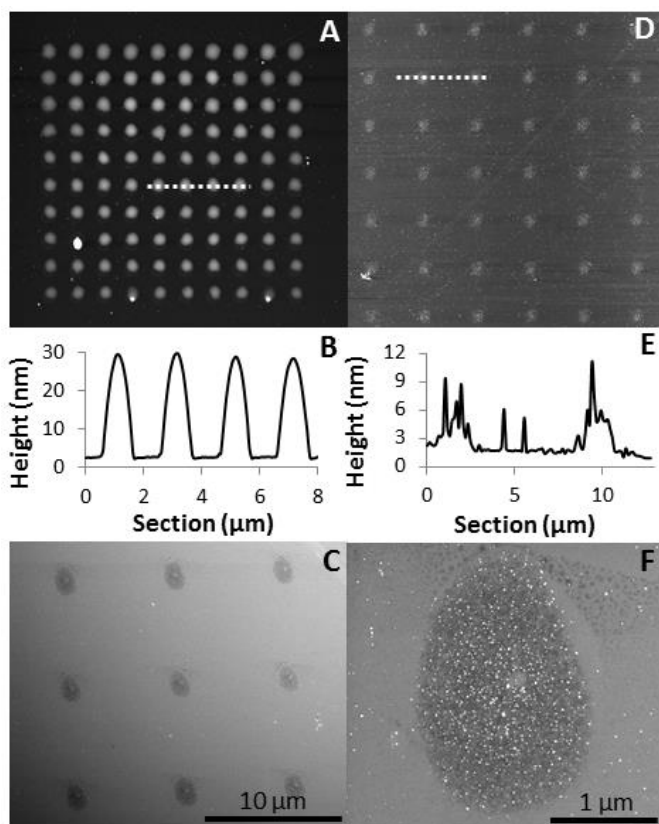


Fig. 3 (A) AFM image of a PDA dot array as-deposited. (B) Height profile corresponding to the line in panel A. (D) AFM image of a PDA dot array after the in-situ reduction of Ag. (E) Height profile corresponding to the line in panel D. (C, F) SEM images of the PDA motifs after the in-situ reduction of Ag.

This work was partly funded through grants MAT2012-38318-C03-02 and MAT2012-38319-C02-01 of the Spanish MINECO. M.G. thanks the CSIC for a JAEPre predoctoral grant. We thank the ICN2 Common Services and Equipment team and Electron Microscopy division. We also thank Dr. A. Lostao and M. C. Pallarés from the Instituto de Nanociencia de Aragón (INA) for technical help.

Notes and references

^a ICN2 - Institut Català de Nanociència i Nanotecnologia, Campus UAB, 08193 Bellaterra (Barcelona), Spain CSIC

CSIC - Consejo Superior de Investigaciones Científicas, ICN2 Building, Campus UAB, 08193 Bellaterra (Barcelona), Spain

E-mail: druiz@cin2.es.

Electronic Supplementary Information (ESI) available: [Experimental details, spectroscopic characterization and additional images]. See DOI: 10.1039/c000000x/

1. X. Duan, Y. Zhao, E. Berenschot, N. R. Tas, D. N. Reinhoudt, and J. Huskens, *Adv. Funct. Mater.*, 2010, **20**, 251.
2. Y. Lei, S. Yang, M. Wu, and G. Wilde, *Chem. Soc. Rev.*, 2011, **40**, 1247.
3. Y. Xia and G. M. Whitesides, *Annu. Rev. Mater. Sci.*, 1998, **28**, 153.
4. S. R. Whaley, D. S. English, E. L. Hu, P. F. Barbara, and A. M. Belcher, *Nature*, 2000, **405**, 665.
5. H. Lee, S. M. Dellatore, W. M. Miller, and P. B. Messersmith, *Science*, 2007, **318**, 426.
6. J. Sedó, J. Saiz-Poseu, F. Busqué, and D. Ruiz-Molina, *Adv. Mater.*, 2013, **25**, 653.
7. Y. Liu, K. Ai, and L. Lu, *Chem. Rev.*, 2014, **114**, 5057.
8. I. You, S. M. Kang, S. Lee, Y. O. Cho, J. B. Kim, S. B. Lee, Y. S. Nam, and H. Lee, *Angew. Chem. Int. Ed.*, 2012, **51**, 6126.
9. S. H. Ku, J. S. Lee, and C. B. Park, *Langmuir*, 2010, **26**, 15104.
10. R. Ogaki, D. T. Bennetsen, I. Bald, and M. Foss, *Langmuir*, 2012, **28**, 8594.
11. K. Sun, Y. Xie, D. Ye, Y. Zhao, Y. Cui, F. Long, W. Zhang, and X. Jiang, *Langmuir*, 2012, **28**, 2131–.
12. E. Bellido, I. Ojea-Jiménez, A. Ghirri, C. Alvino, A. Candini, V. Puntès, M. Affronte, N. Domingo, and D. Ruiz-Molina, *Langmuir*, 2012, **28**, 12400.
13. E. Bellido, S. Cardona-Serra, E. Coronado, and D. Ruiz-Molina, *Chem. Commun.*, 2011, **47**, 5175.
14. H. Lee, N. F. Scherer, and P. B. Messersmith, *Proc. Natl. Acad. Sci. U. S. A.*, 2006, **103**, 12999.
15. M. Guardingo, E. Bellido, R. Miralles-Llumà, J. Faraudo, J. Sedó, S. Tatay, A. Verdager, F. Busqué, and D. Ruiz-Molina, *Small*, 2014, **10**, 1594.
16. F. Bernsmann, A. Ponche, C. Ringwald, J. Hemmerlé, J. Raya, B. Bechinger, J. Voegel, P. Schaaf, and V. Ball, *J. Phys. Chem. C*, 2009, **113**, 8234.
17. F. K. Yang and B. Zhao, *Open Surf. Sci. J.*, 2011, **3**, 115.
18. H.-W. Chien, W.-H. Kuo, M.-J. Wang, S.-W. Tsai, and W.-B. Tsai, *Langmuir*, 2012, **28**, 5775.
19. S. Saidin, P. Chevallier, M. R. Abdul Kadir, H. Hermawan, and D. Mantovani, *Mater. Sci. Eng. C. Mater. Biol. Appl.*, 2013, **33**, 4715.
20. V. Ball, I. Nguyen, M. Haupt, Ch. Oehr, C. Arnoult, V. Toniazzon, D. Ruch, *J. Colloid Interface Sci.* 2011, **364**, 359.
21. S. S. Hong, Y. S. Na, S. Choi, I. T. Song, W. Y. Kim and H. Lee, *Adv. Funct. Mater.*, 2012, **22**, 4711.

22. S. Hong, J. S. Lee, J. Ryu, S. H. Lee, D. Y. Lee, D.-P. Kim, C. B. Park, and H. Lee, *Nanotechnology*, 2011, **22**, 494020.